RSC Advances

COMMUNICATION

View Article Online
View Journal | View Issue

Cite this: *RSC Adv.*, 2014, **4**, 51619

Received 10th September 2014
Accepted 7th October 2014

DOI: 10.1039/c4ra10130h

www.rsc.org/advances

One-pot synthesis of thin $Co(OH)_2$ nanosheets on graphene and their high activity as a capacitor electrode†

Gyoung Hwa Jeong,‡[a] Hae-Min Lee,‡[b] Heewoong Lee,[c] Chang-Koo Kim,[b] Yuanzhe Piao,[d] Jae-Hyeok Lee,[c] Jae-Ho Kim[c] and Sang-Wook Kim*[ac]

We synthesized $Co(OH)_2$/graphene composites from graphite without a graphene oxide (GO) step. The $Co(OH)_2$/graphene composite exhibited a specific capacitance of 960 F g^{-1} at a current density of 10 A g^{-1}. In addition, after 5000 cycles of charge/discharge operation, the $Co(OH)_2$/graphene composite maintained its initial specific capacitance value of 93.4% at a current density of 30 A g^{-1}.

Supercapacitors, a type of energy-storage system, have attracted considerable attention because of their high power capability, long cycle stability, and relatively low cost.[1–3] Because supercapacitors deliver energy at high charge–discharge rates, it is hypothesized that they have higher power density than batteries or fuel cells.[4] Based on the working mechanism, there are two types of supercapacitors: (i) electric double-layer capacitor (EDLC), which has high capacitance due to charge accumulation at the electrode–electrolyte interface and (ii) the redox capacitor, which has a pseudo-capacitance due to the oxidation–reduction reaction.[5] In pseudo-capacitors, metal oxides, including RuO_2,[6] MnO_2,[7] Co_3O_4,[8] NiO,[9] SnO_2,[10] Fe_3O_4,[11] and V_2O_5,[12] have been employed as the electroactive materials. However, single metal oxides usually have some limitations such as poor electrical conduction, insufficient electrochemical cycling stability, limited voltage operating window, and low specific capacitance.[13] To improve supercapacitor functionality, a great deal of research has been conducted on electrode materials because the capacitance and energy density of supercapacitors are highly dependent on the electrode materials.[14,15]

Carbon-based materials have been extensively studied as potential candidates for improving the electrical properties of energy devices, including EDLC.[16,17] Among the studied carbon-based materials, graphene has attracted the greatest interest as a promising electrode material for supercapacitors. Graphene has excellent conductivity, and a high surface area due to its one-atom thick, two-dimensional sp^2 carbon arrangement.[18] Chen *et al.*[19] fabricated supercapacitor electrodes using good quality graphene materials and investigated their performance. They obtained a maximum specific capacitance of 205 F g^{-1} at 1.0 V with an energy density of 28.5 W h g^{-1} in an aqueous electrolyte. This is the best result reported to date for supercapacitors using graphene materials, and it is also significantly higher than the specific capacitance of CNT-based supercapacitors. Ruoff *et al.*[20] succeeded in the chemical synthesis of graphene with a specific surface area of 3100 m^2 g^{-1} that delivered a capacitance of 166 F g^{-1} at various current rates in an organic electrolyte.

Graphene is usually synthesized by reducing chemically exfoliated graphene oxide (GO) with a reducing agent.[21] The loss of oxygen-containing groups during the chemical reduction results in the aggregation of graphene layers. This re-stacking hinders the electrolyte ion access to the surface of the reduced GO (rGO) and decreases the surface area. To avoid the re-stacking, graphene-based composites with various metal oxide such as $Ni(OH)_2$, Mn_3O_4, MnO_2, and Co_3O_4 have been frequently reported.[22–25] In every case, the shape of metal oxide was nano-sized particles. Although the specific capacitances of these graphene-based composites were enhanced, they were not enough to be useful in practical applications. Here, we report a direct method to produce large-scale graphene-based composites from graphite, as a result, graphene surface has no oxygen functional group including hydroxyl, epoxy, and carboxyl group. In addition, our composite has thin $Co(OH)_2$ nanosheet, not nanoparticles, which result in improved activity. The resulting graphene layers were not aggregated (re-stacked) and would be suitable for use in electrode materials. The following is a brief description of the fabrication process. First, using sonication and stirring graphite with sodium dodecyl sulfate (SDS), we

[a]*Center of Molecular Science and Technology, Ajou University, Suwon 443-749, Korea*
[b]*Division of Energy Systems Research, Ajou University, Suwon 443-749, Korea*
[c]*Department of Molecular Science and Technology, Ajou University, Suwon 443-749, Korea. E-mail: swkim@ajou.ac.kr; Fax: +82 31 219 1592; Tel: +82 31 219 2522*
[d]*Graduate School of Convergence Science and Technology, Seoul National University, Suwon, 443-270, Korea*

† Electronic supplementary information (ESI) available. See DOI: 10.1039/c4ra10130h

‡ These authors contributed equally.

prepared SDS-functionalized graphene flakes. Cobalt precursors were then added to the solution, and the solution was aged under basic hydrothermal conditions. The complete experimental details are available in the Experimental section. The synthesized samples were characterized by transmission electron microscopy (TEM), powder X-ray diffraction (XRD), and Barrett–Emmett–Teller (BET) methods. In addition, we measured the electrochemical properties of the electrode materials for supercapacitors.

The $Co(OH)_2$ nanosheets were synthesized between the SDS functionalized graphene flakes by the hydrothermal method. Recently, we reported the direct synthesis of noble metal/graphene composites using photosynthesis.[26] Although this method was very simple, it was impossible to form metal oxide/graphene composites. In the new procedure, sonication of graphite and SDS showed a number of crumpling and scrolling (>10 layers, see Fig. S1†). Then, Co ions were selectively adsorbed on the graphene flakes because of the electrostatic interactions between the anionic surfactants and the cobalt ions. Subsequently, the $Co(OH)_2$ nanosheets were formed utilizing a highly basic hydrothermal condition with NaOH. (See Fig. 1) Fig. 2a–c show the TEM images of the synthesized $Co(OH)_2$/graphene composites at different magnifications. These figures show well-dispersed nanosheets on the graphene. In Fig. 2a and b, the $Co(OH)_2$ consist of flower-like aggregates made of intertangled thin nanosheets with dimension on the graphene surface. In particular, Fig. 1c shows very thin and wrinkled $Co(OH)_2$ nanosheets. Fig. 1d shows the lattice planes are approximately 0.236 nm corresponding to the interplanar distance of the $Co(OH)_2$ (011) plane, as confirmed by XRD (Fig. 3a). All of the diffraction peaks can be indexed as hexagonal $Co(OH)_2$ with lattice constants $a = 3.176$ Å and $c = 4.614$ Å in agreement with the literature values (JCPDS 30-0443).[27] To investigate the $Co(OH)_2$ nanosheet structure on graphene, we used high-angle annular dark-field scanning TEM (HAADF-STEM). (Fig. 2e) From the nanoscale mapping images, we could confirm that the distributions of carbon and cobalt are equal in chosen area, which confirms the presence of the $Co(OH)_2$ nanosheet on the graphene surface. In addition, from atomic force microscopy (AFM), we observed that the thickness of the synthesized $Co(OH)_2$ nanosheet and graphene are approximately 15 and 2 nm, respectively. (Fig. S2†) As we stated above, an electrochemically active surface is an important factor for improving the specific capacitance in various carbon electrode materials. Therefore, we measured the surface area using

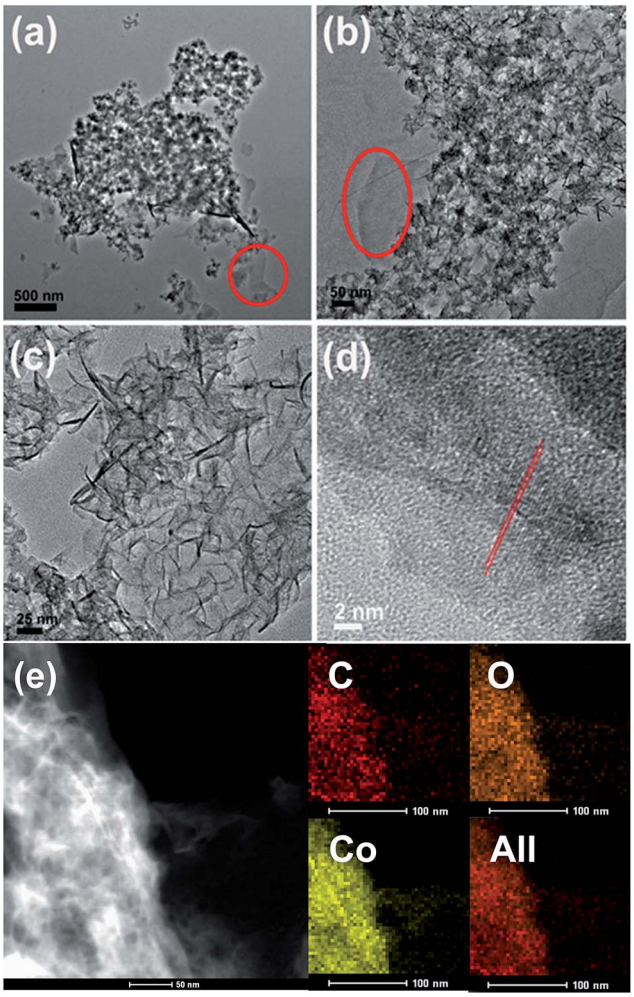

Fig. 2 TEM images of $Co(OH)_2$/graphene nanocomposites. Red circles in (a) and (b), show graphene. (c) and (d) magnified image of $Co(OH)_2$ nanosheets on graphene Lattice distance of $Co(OH)_2$ is 0.236 nm. (e) HAADF-STEM mapping images of $Co(OH)_2$ nanosheets on graphene.

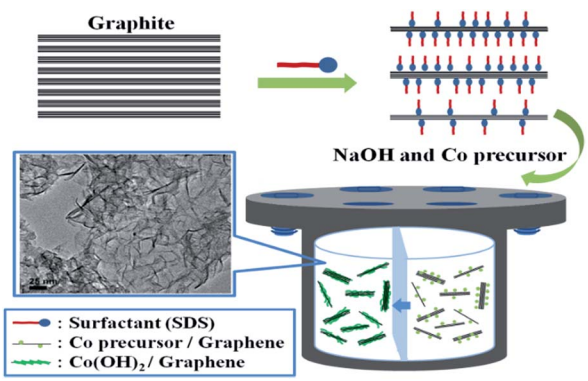

Fig. 1 Synthesis of $Co(OH)_2$/graphene composites from graphite.

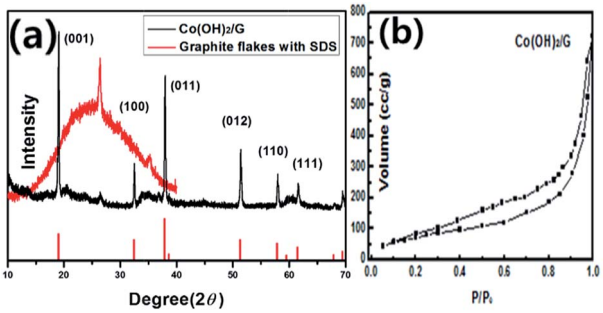

Fig. 3 (a) XRD patterns of $Co(OH)_2$/graphene nanocomposites and graphene flakes functionalized SDS. Red peaks are the reference of $Co(OH)_2$. (JCPDS no. 30-0443) (b) Nitrogen adsorption/desorption isotherms distribution of $Co(OH)_2$/graphene nanocomposites.

the BET gas-sorption method. Fig. 3b shows the nitrogen adsorption/desorption isotherm of the $Co(OH)_2$/graphene. The BET specific surface area of the prepared sample was 287.23 $m^2\ g^{-1}$, which is nine times larger than that of graphite (31.38 $m^2\ g^{-1}$), as shown in Fig. S3.† In comparison experiments, we could not observe the nanosheets using the above experimental procedure in the absence of graphene, although we could confirm that $Co(OH)_2$ was formed. (Fig. S4†) Additionally, when we performed the same experiment using GO, different Co_3O_4 was synthesized instead of $Co(OH)_2$. (Fig. S5†) We suppose that the oxygen groups of GO affect the formation reaction of Co_3O_4.

The electrochemical experiments and calculation details has been provided in the ESI.† Fig. 4a shows the cyclic voltammograms (CVs) of the $Co(OH)_2$ and $Co(OH)_2$/graphene at scan rates of 100 mV s^{-1}. Their CVs were measured and compared using Ag/AgCl as a reference in 2 M KOH electrolyte solution. Nearly symmetric CVs for both have redox peaks, which indicate good electrochemical capacitive nature. The redox reactions are as follows:[28–30]

$$Co(OH)_2 + OH^- \leftrightarrow CoOOH + H_2O + e^- \quad (1)$$

$$CoOOH + OH^- \leftrightarrow CoO_2 + H_2O + e^- \quad (2)$$

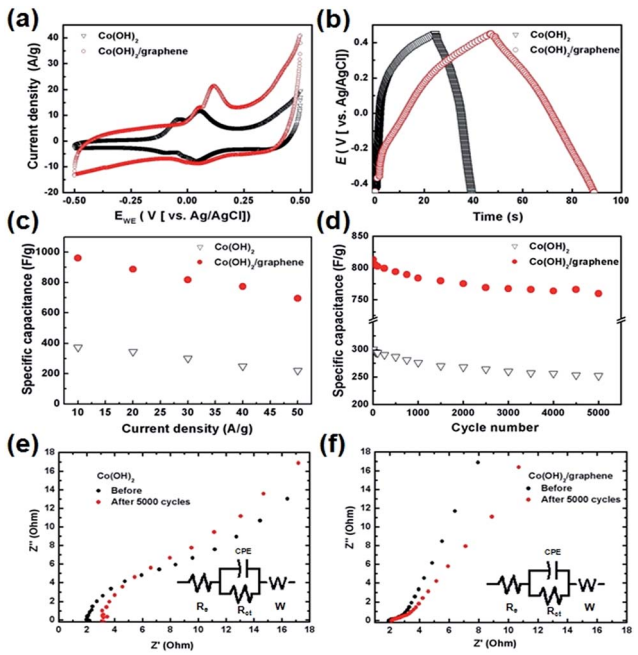

Fig. 4 (a) Cyclic voltammetry (CV) curves of $Co(OH)_2$ and $Co(OH)_2$/graphene at 100 mV s^{-1} in 2 M KOH solution. (b) Galvanostatic charge/discharge behaviors of $Co(OH)_2$ and $Co(OH)_2$/graphene electrodes at a constant current density 10 A g^{-1} in 2 M KOH solution. (c) Specific capacitance of $Co(OH)_2$ and $Co(OH)_2$/graphene electrodes in the range of current density 10 to 50 A g^{-1}. (d) Cycling life of $Co(OH)_2$ and $Co(OH)_2$/graphene at a constant current density 30 A g^{-1} in 2 M KOH solution. Nyquist plots of (e) the $Co(OH)_2$ and (f) $Co(OH)_2$/graphene electrode before/after 5000 cycles in the 2 M KOH solution at a current density of 10 A g^{-1}.

The CVs of both the $Co(OH)_2$ and $Co(OH)_2$/graphene electrodes show two pairs of symmetric potential peaks that are attributed to the redox reactions (1) and (2) at a high scan rate of 100 mV s^{-1}. Unlike the curve of $Co(OH)_2$, the anodic and cathodic peaks of $Co(OH)_2$/graphene electrode shifted toward positive potential and negative potential, respectively. The $Co(OH)_2$/graphene electrode had a high current density in the same potential window rather than the $Co(OH)_2$ electrode and the CV curve of the $Co(OH)_2$/graphene electrode had a nearly rectangular shape which is characteristic of an EDLC in the potential range from −0.5 to 0.5 V due to the existence of graphene nanosheets. (Fig. 4a) Fig. 4b shows the first charge–discharge profiles of the $Co(OH)_2$ and $Co(OH)_2$/graphene electrodes between −0.45 and 0.45 V (*vs.* Ag/AgCl) at a galvanostatic current density of 10 A g^{-1} in 2 M KOH solution. The shape of the charge/discharge curves shows a typical pseudocapacitive behavior,[31] which is in agreement with the CV result. The $Co(OH)_2$/graphene electrode shows a more symmetric triangular shape during the charge/discharge processes and has a longer discharge time which is roughly three times than that of the $Co(OH)_2$ electrode. In previously reported results, the graphene as a conductive carbon improved the electrode properties considerably, also, in our case, the effect is predominant. Utilizing the charge/discharge measurements, the specific capacitance of the $Co(OH)_2$ and $Co(OH)_2$/graphene electrodes was calculated using the following equation:

$$SC_{CD} = \frac{I \times t}{m \times \Delta V} \text{ (see Experimental section)}$$

Fig. 4c shows the specific capacitance of the $Co(OH)_2$ and $Co(OH)_2$/graphene at various current densities ranging from 10 to 50 A g^{-1}. As the current density increased from 10 to 50 A g^{-1}, the specific capacitance gradually decreased. The specific capacitance of the $Co(OH)_2$ and $Co(OH)_2$/graphene had a maximum value of 372 and 960 F g^{-1}, respectively, at a current density of 10 A g^{-1} and a minimum value of 220 and 694 F g^{-1}, respectively, at a current density of 50 A g^{-1}. Compared to 372 F g^{-1} for pure $Co(OH)_2$, the capacitance of $Co(OH)_2$/graphene nanosheet is remarkably enhanced, which is also higher than that of $Co(OH)_2$ nanoparticle and reduced graphene oxide composite.[14] We investigated the electrochemical behavior of rGO sheet made by modified Hummer's method. The specific capacitance of rGO had ~135 F g^{-1} in aqueous electrolyte. This result show that the capacitance of our $Co(OH)_2$/graphene is higher than that of $Co(OH)_2$ and rGO. Recent studies of the nanostructured cobalt hydroxide prepared by hydrothermal method reported specific capacitances of 298–589 F g^{-1} using cobalt hydroxide and 330–622 F g^{-1} using pyrolytic graphite or graphene.[32–36] To evaluated the stability of the $Co(OH)_2$ and $Co(OH)_2$/graphene, the charge–discharge cycling test at a current density of 30 A g^{-1} was performed. Fig. 4d shows the cycling stability of the $Co(OH)_2$ and $Co(OH)_2$/graphene electrodes. The specific capacitance of the $Co(OH)_2$ and $Co(OH)_2$/graphene first decreased by approximately 8% and 5%, respectively, during the initial 1000 cycles, and then it decreased slightly and stable during the next 4000 cycles. After

5000 cycles of the charge–discharge operation, they retained 84 and 93.4% of their initial specific capacitance value, respectively. During the cycling process, aggregation which could lead to the decrease of electro-active site and specific surface area or restacking inevitably occurs in graphene because of the inter sheet van der Waals attractions.[37,38] However, $Co(OH)_2$/graphene maintained their initial capacitance properties, which indicate potentially no restacking and aggregation of graphene sheets and inhibiting the volume change and detachment of the $Co(OH)_2$. We estimate the reason is because of their unique structure such that $Co(OH)_2$ nanosheets were sandwiched between graphene layers. To investigate the resistance between electrode/electrolyte interface as well as the internal resistance of the electrode material, the electrochemical impedance spectroscopy (EIS) measurements were performed from 100 kHz to 0.05 kHz (Fig. 4e and f). The Nyquist plot of the $Co(OH)_2$ and $Co(OH)_2$/graphene electrodes in all the electrolytes consist of the high frequency semicircles and inclined lines in low frequency. The electrode series resistance (R_e) indicated a combinational resistance of ionic resistance of electrolyte, intrinsic resistance of substrate, and contact resistance at the active material/current collector interface was derived from the high frequency intersection of the Nyquist plot in the real part (Z') axis.[19] Before cycle test, $Co(OH)_2$ and $Co(OH)_2$/graphene electrodes have similar starting R_e values, 2.22 and 1.92 Ω, respectively. However, after 5000 cycling, the R_e value of $Co(OH)_2$ electrode increased by 3.44 Ω, while the R_e value of $Co(OH)_2$/graphene electrode was 2.09 Ω. (Fig. 4e and f) It confirmed that the electronic conductivity of $Co(OH)_2$/graphene was superior to that of $Co(OH)_2$ electrode. Meanwhile, a big semi-arc was found for the $Co(OH)_2$ electrode. The semicircle in the high frequency range corresponds to the charge transfer resistance (R_{ct}), and the constant phase capacitance (CPE) caused by Faradaic reactions and the double layer capacitance on the grain surface layer.[19] The R_{ct} value of $Co(OH)_2$ and $Co(OH)_2$/graphene was estimated 8.46 and 2.51 Ω, respectively. After 5000 cycling, however, the R_{ct} value of $Co(OH)_2$ increased 9.77 Ω, which is much larger than that of $Co(OH)_2$/graphene, with only 3.19 Ω. Evidently, it indicates that the graphene nanosheet minimized the interfacial resistance of the charge transfer process. In the low frequency range, the straight sloping line represents the Warburg resistance (W) related to the electrolyte diffusion process and OH– ion diffusion into electrode.[20] Consequently, the remarkable enhancement in specific capacitance is attributed to the graphene nanosheets.

Conclusions

We report the synthesis of $Co(OH)_2$ nanosheets on graphene prepared directly from graphite; we expected that the activity of the composite is better than that from graphene composite which is reduced chemically with $NaBH_4$, hydrazine and so on. The synthesized composite was tested as an electrode material for supercapacitors. Compared with previous studies, the specific capacitance value of our $Co(OH)_2$/graphene composite is better, which is 960 F g^{-1} at a current density of 10 A g^{-1}. Furthermore, after 5000 charge–discharge cycles at a current density of 30 A g^{-1}, the $Co(OH)_2$/graphene retained 93.4% of its initial specific capacitance. Because of the sandwich structure of $Co(OH)_2$/nanosheets and grapheme, there is little restacking and aggregation.

Acknowledgements

This work was supported by the National Research Foundation of Korea (NRF) grant no. 2014R1A5A1009799, 2013R1A1A2A10008031, 2012-004416, the Priority Research Program (2009-0093826), S-Oil Corporation, and an Ajou University Research Centers fellowship of 2010 (Grant no. S-2010-G0001-00058).

Notes and references

1 H. Wang and H. Dai, *Chem. Soc. Rev.*, 2013, **42**, 3088.
2 N. S. Choi, Z. Chen, S. A. Freunberger, X. Ji and Y. K. Sun, *Angew. Chem., Int. Ed.*, 2012, **51**, 9994.
3 Z. Lei, Z. Liu, H. Wang, X. Sun, L. Lu and X. S. Zhao, *J. Mater. Chem. A*, 2013, **1**, 2313.
4 Y. Li, M. V. Zijll, S. Chiang and N. Pan, *J. Power Sources*, 2011, **196**, 6003.
5 G. Wang, L. Zhang and J. Zhang, *Chem. Soc. Rev.*, 2012, **41**, 797.
6 J. P. Zheng, P. J. Cygan and T. R. Jow, *J. Electrochem. Soc.*, 1995, **142**, 2699.
7 S. C. Pang, M. A. Anderson and T. W. Chapman, *J. Electrochem. Soc.*, 2000, **147**, 444.
8 C. W. Kung, H. W. Chen, C. Y. Lin, R. Vittal and K. C. Ho, *J. Power Sources*, 2012, **214**, 91.
9 Y. Y. Xi, D. Li, A. B. Djurišić, M. H. Xie, K. Y. K. Man and W. K. Chan, *Electrochem. Solid-State Lett.*, 2008, **11**, D56.
10 S. N. Pusawale, P. R. Deshmukh and C. D. Lokhande, *Appl. Surf. Sci.*, 2011, **257**, 9498.
11 J. Chen, K. Huang and S. Liu, *Electrochim. Acta*, 2009, **55**, 1.
12 Q. T. Qu, Y. Shi, L. L. Li, W. L. Guo, Y. P. Wu, H. P. Zhang, S. Y. Guan and R. Holze, *Electrochem. Commun.*, 2009, **11**, 1325.
13 F. Ebrahimi, in *Nanocomposites – New Trends and Developments*, Tech Publisher, Croatia, 2012.
14 M. Jayalakshmi, M. M. Rao, N. Venugopal and K. B. Kim, *J. Power Sources*, 2007, **166**, 578.
15 J. Zang and X. Li, *J. Mater. Chem.*, 2011, **21**, 10965.
16 X. Du, C. Wang, M. Chen, Y. Jiao and J. Wang, *J. Phys. Chem. C*, 2009, **113**, 2643.
17 Z. L. Wang, D. Xu, H. G. Wang, Z. Wu and X. B. Zhang, *ACS Nano*, 2013, **7**, 2422.
18 Z. Lei, N. Christov and X. S. Zhao, *Energy Environ. Sci.*, 2011, **4**, 1866.
19 Y. Wang, Z. Shi, Y. Huang, Y. Ma, C. Wang, M. Chen and Y. Chen, *J. Phys. Chem. C*, 2009, **113**, 13103.
20 Y. Zhu, S. Murali, M. D. Stoller, K. J. Ganesh, W. Cai, P. J. Ferreira, A. Pirkle, R. M. Wallace, K. A. Cychosz, M. Thommes, D. Su, E. A. Stach and R. S. Ruoff, *Science*, 2011, **332**, 1537.

21 J. Zhang, H. Yang, G. Shen, P. Cheng, J. Zhang and S. Guo, *Chem. Commun.*, 2010, **46**, 1112.
22 J. Yan, Z. Fan, W. Sun, G. Ning, T. Wei, Q. Zhang, R. Zhang, L. Zhi and F. Wei, *Adv. Funct. Mater.*, 2012, **22**, 2632.
23 B. Wang, J. Park, C. Wang, H. Ahn and G. Wang, *Electrochim. Acta*, 2010, **55**, 6812.
24 S. Chen, J. Zhu, X. Wu, Q. Han and X. Wang, *ACS Nano*, 2010, **4**, 2822.
25 G. He, J. Li, H. Chen, J. Shi, X. Sun, S. Chen and X. Wang, *Mater. Lett.*, 2012, **82**, 61.
26 G. H. Jeong, S. H. Kim, M. Kim, D. Choi, J. H. Lee, J. H. Kim and S. W. Kim, *Chem. Commun.*, 2011, **47**, 12236.
27 S. Chen, J. Zhu and X. Wang, *J. Phys. Chem. C*, 2010, **114**, 11829.
28 Y. Chen, X. Zhang, H. Zhang, X. Sun, D. Zhang and Y. Ma, *RSC Adv.*, 2012, **2**, 7747.
29 C. Yuan, X. Zhang, B. Gao and J. Li, *Mater. Chem. Phys.*, 2007, **101**, 148.
30 V. Gupta, T. Kusahara, H. Toyama, S. Gupta and N. Miura, *Electrochem. Commun.*, 2007, **9**, 2315.
31 B. E. Conway, *J. Electrochem. Soc.*, 1991, **138**, 1539.
32 C. Yuan, X. Zhang, L. Hou, L. Shen, D. Li, F. Zhang, C. Fan and J. Li, *J. Mater. Chem.*, 2010, **20**, 10809.
33 F. Cao, G. X. Pan, P. S. Tang and H. F. Chen, *J. Power Sources*, 2012, **216**, 395.
34 Y. Q. Zhang, X. H. Xia, J. Kang and J. P. Tu, *Chin. Sci. Bull.*, 2012, **57**, 4215.
35 J. Jiang, J. Liu, R. Ding, J. Zhu, Y. Li, A. Hu, X. Li and X. Huang, *Appl. Mater. Interfaces*, 2011, **3**, 99.
36 C. Y. Sun, Y. G. Zhu, T. J. Zhu, J. Xie, G. S. Cao and X. B. Zhao, *J. Solid State Electrochem.*, 2013, **17**, 1159.
37 J. Xie, Y. X. Zheng, S. Y. Liu, W. T. Song, Y. G. Zhu, G. S. Cao, T. J. Zhu and X. B. Zhao, *Int. J. Electrochem. Sci.*, 2012, **7**, 1319.
38 Y. Sun, Q. Wu and G. Shi, *Energy Environ. Sci.*, 2011, **4**, 1113.